Ultrasound in Med. & Biol., Vol. 37, No. 2, pp. 289–300, 2011

0301-5629/$ - see front matter

ELSEVIER

doi:10.1016/j.ultrasmedbio.2010.10.020

● *Original Contribution*

MEASUREMENT OF THE ULTRASOUND ATTENUATION AND DISPERSION IN WHOLE HUMAN BLOOD AND ITS COMPONENTS FROM 0–70 MHZ

Bradley E. Treeby,* Edward Z. Zhang,* Alison S. Thomas,† and Ben T. Cox*

*Department of Medical Physics and Bioengineering, University College London, London, United Kingdom; and †Department of Clinical Haematology, University College London Hospital, London, United Kingdom

(*Received* 9 *September* 2010; *revised* 13 *October* 2010; *in final form* 15 *October* 2010)

Abstract—The ultrasound attenuation coefficient and dispersion from 0–70 MHz in whole human blood and its components (red blood cells and plasma) at 37°C is reported. The measurements are made using a fixed path substitution technique that exploits optical mechanisms for the generation and detection of ultrasound. This allows the measurements to cover a broad frequency range with a single source and receiver. The measured attenuation coefficient and dispersion in solutions of red blood cells and physiological saline for total haemoglobin concentrations of 10, 15 and 20 g/dL are presented. The attenuation coefficient and dispersion in whole human blood taken from four healthy volunteers by venipuncture is also reported. The power law dependence of the attenuation coefficient is shown to vary across the measured frequency range. This is due to the varying frequency dependence of the different mechanisms responsible for the attenuation. The attenuation coefficient measured at high frequencies is found to be significantly higher than that predicted by historical power law parameters. A review of the attenuation mechanisms in blood along with previously reported experimental measurements is given. Values for the sound speed and density in the tested samples are also presented. (E-mail: btreeby@mpb.ucl.ac.uk) © **2011 World Federation for Ultrasound in Medicine & Biology.**

Key Words: **Ultrasound attenuation, Absorption mechanisms, Relaxation absorption, Viscous relative motion, Human blood.**

INTRODUCTION

Broadband measurement of tissue properties

The accurate acoustic characterisation of biologic tissue has been a subject of interest to acousticians and sonographers for more than half a century (Duck 1990). These properties provide the intrinsic contrast between the biologic structures, tissue types, physiological states and pathologies that can be detected using ultrasound. The characteristics of blood are of particular relevance due to the multitude of functional, physiological, rheological and pathological parameters that can be extracted from its acoustic properties. In this context, knowledge of the acoustic attenuation coefficient in blood has been used for arterial ultrasound imaging (Lockwood et al. 1991; Hoskins 2007), ultrasound analysis of blood clotting (Huang et al. 2005; Libgot-Callé et al. 2009), ultrasonic measurement of blood haematocrit (Secomski et al. 2009) and the diagnosis of various blood disorders (Shung and Reid 1979).

Address correspondence to: Bradley E. Treeby, Department of Medical Physics and Bioengineering, University College London, Gower Street, London, WC1E 6BT United Kingdom. E-mail: btreeby@mpb.ucl.ac.uk

The recent development of high resolution ultrasound imaging technologies, such as ultrasound biomicroscopy (Foster et al. 2000) and photoacoustic tomography (Treeby et al. 2010), has provided a renewed interest in characterising tissue properties beyond the range of historical measurements made at conventional diagnostic ultrasound frequencies. There is a similar interest from researchers working in treatment planning for high-intensity focused ultrasound, as both nonlinear wave propagation and acoustic cavitation can generate ultrasound frequencies outside the traditional diagnostic range (ter Haar and Coussios 2007). While more than 30 publications have reported frequency dependent measurements of the acoustic attenuation coefficient in blood since Carstensen's seminal papers more than 50 years ago (see Table 1), none of these report broadband measurements in human blood at physiological temperatures and concentrations.

Here, the sound speed, density, ultrasound attenuation coefficient and dispersion (variation of the sound speed with frequency) from 0–70 MHz in whole human blood and its components (red blood cells and plasma) at 37°C are reported. The format of the article is as follows. First, the composition of blood and the various

Table 1. Measurements of the frequency dependent acoustic attenuation in blood and red blood cell (RBC) or haemoglobin (Hb) suspensions reported in the literature

Reference	Sample	Conc	Temp [°C]	Freq [MHz]
Carstensen et al. (1953)	Human RBC in plasma	0–85%	–	0.8–3
Carstensen and Schwan (1959a)	Bovine RBC in plasma	40%	25	0.7–10
Carstensen and Schwan (1959a)	Bovine RBC in saline	13–95%	25	0.7–10
Carstensen and Schwan (1959b)	Human Hb solutions	4–30 g/dL	7–35	0.5–10
Edmonds (1962)	Bovine Hb solutions	4–33 g/dL	5–25	32–232
Schneider et al. (1969)	Bovine Hb solutions	8–18 g/dL	8–25	0.5–1000
Edmonds et al. (1970)	Bovine Hb solutions	15 g/dL	25	10–130
Woodcock (1970)	Human RBC in saline	–	–	6–10
White and Slutsky (1971)	Bovine Hb solutions	15 g/dL	0	3–70
O'Brien Jr. and Dunn (1972)	Bovine Hb solutions	–	10	0.3–50
White and Slutsky (1972)	Bovine Hb solutions	0.0023 M	0	5–50
Kikuchi et al. (1972)	Whole human blood	47%	37	2–10
Kremkau et al. (1973)	Fixed bovine RBC	–	25	5–90
Shung and Reid (1977)	Whole human blood	8.7 g/dL	22	7–10
Hughes et al. (1979)	Canine RBC in plasma	0–53%	37	10
Narayana et al. (1984)	Whole human blood	–	22	4.8
Kremkau and Cowgill (1984)	Hb solutions	8.5 g/dL	22	1–90
Kremkau and Cowgill (1985)	Hb solutions	5 g/dL	21–22	1–90
Kremkau (1988)	Hb solutions	9–21 g/dL	20–22	1–90
Yuan and Shung (1988)	Porcine RBC in plasma	11–47%	23	3.5–12.5
Dai and Feng (1988)	Bovine RBC in saline	17%	–	2–6
Barnes et al. (1988)	Bovine Hb solutions	2–15 g/dL	20	0.2–1.2
Lockwood et al. (1991)	Human RBC in saline	44%	–	30–60
Wang and Shung (1997)	Porcine RBC in saline	5–45%	room	5–30
Secomski et al. (2001)	Whole human blood	24–52%	37	16, 20
Maruvada et al. (2002)	Porcine RBC in saline	6–30%	–	30–90
Stride and Saffari (2004)	Whole human blood	–	29	3–5
Hughes et al. (2005)	Whole porcine blood	40%	37	2–8
Dukhin et al. (2006)	Human RBC in plasma	9–95%	–	2–100
Liu et al. (2010)	Whole bovine and pig blood	–	20–95	5–12

Concentrations are given in their measured units, either as haematocrit [%], total haemoglobin concentration [g/dL] or molar haemoglobin concentration [M].

attenuation mechanisms are reviewed. The measurement system and experimental procedure are then described and the measurement results presented and discussed. These are compared with experimental data previously reported in the literature. Summary and discussion are then given.

Blood composition

Under normal physiological conditions, human blood consists of blood cells (approximately 45% by volume) suspended in plasma. The blood cells are made up largely of red blood cells (erythrocytes) with small proportions of platelets (thrombocytes) and white blood cells (leukocytes). Published normal ranges for cell counts vary slightly with patient population and method of analysis. Normal ranges in a Caucasian population demonstrate a red cell count of $4.32-5.66\times10^{12}$ cells/L in men and $3.88-4.99\times10^{12}$ cells/L in women, a leukocyte count of $3.7-9.5\times10^{9}$ cells/L in men and $3.9-11.1\times10^{9}$ cells/L in women (Bain 2006) and a platelet count of $165-396\times10^{9}$ cells/L (Giacomini et al. 2001). The proportion of the total volume of whole blood that red blood cells occupy (commonly called the packed cell volume or haematocrit) is normally in the range 39%–51% for males and 36%–48% for females (Fairbanks and Tefferi 2000, 2001). The red blood cells themselves are densely packed with the oxygen carrying protein haemoglobin, with the normal range for the total haemoglobin concentration in whole blood 13.3−16.7 g/dL for males and 11.8−14.8 g/dL for females (Bain 2006). If the blood cells are removed from whole blood by centrifugation, the remaining fluid (plasma) is made up of 91% water by weight with three major protein types: albumin (4 g/dL), globulin (2.7 g/dL) and fibrinogen (0.3 g/dL) (Schneck 2003). The remainder of the plasma consists of other minerals, trace elements and lipids.

Ultrasound absorption mechanisms in blood

The acoustic attenuation in whole blood can be attributed to a number of different mechanisms. These occur on both a cellular level (due to the cellular membrane separating the differing intracellular and extracellular fluids) and on a molecular level within the intracellular and extracellular fluids themselves. The molecular level absorption mechanisms include viscosity and thermal conduction (the "classical" relaxation phenomena) along with additional structural and thermal relaxation processes (Bamber 2004). The cellular level absorption mechanisms include viscous relative motion and thermal conduction due to the inhomogeneous

regions of acoustic and thermal properties, in addition to scattering. Before proceeding, it is important to make clear the distinction between the discussion of acoustic absorption (which describes the gradual degradation of acoustic energy into thermal energy) and acoustic attenuation (which also includes the effects of scattering).

Relaxation absorption occurs when there is a cyclical transfer of kinetic energy to other energy states in which there is a characteristic time delay (relaxation time) before the energy is recovered (Herzfeld and Rice 1928). For example, in polyatomic gases, in regions of compression (where there is an increased average molecular motion), some of the acoustic energy is transferred from external translational molecular vibration to internal molecular energy states. When the compression subsides, there is then a time delay before this energy is recovered as kinetic energy. Similarly, the absorption in sea water is in part due to the dissociation and association of magnesium sulphate as the compressions and rarefactions change the local concentration of the ions (Francois and Garrison 1982). If a particular relaxation time is of the same order as the period of the propagating ultrasound wave, the phase difference between the transfer of energy to and from the alternate energy state will cause a net dissipation of energy. Each relaxation process is characterised by a single absorption peak that occurs when this reaction is completely out of phase.

A historic (although somewhat artificial) distinction is sometimes made between the classical relaxation phenomena (viscosity and thermal conduction) and other structural and thermal relaxation processes. Absorption due to viscosity occurs because of the diffusion of momentum between molecules with different particle velocity. This effect is normally characterised by shear and bulk viscosity coefficients, both of which appear in the classical Navier-Stokes equation. However, while the former can be directly measured, the latter (which characterises the absorption due to the stiffness forces that resist compression) is largely a phenomenological term that also encapsulates other absorption mechanisms. For example, in pure water, both shear and bulk viscosity coefficients are required to account for the experimentally observed absorption (Pinkerton 1949; Liebermann 1949). This is due to a structural relaxation mechanism (Hall 1948). However, the convention of assigning this particular absorption to a bulk viscosity coefficient rather than considering it directly as a relaxation process would appear to be largely historic. Consequently, the identification of the particular mechanisms responsible for bulk viscosity is analogous to the identification of the other relaxation processes.

In blood, additional relaxation phenomena are evident due to the presence of proteins such as haemoglobin and albumin. Broadband measurements of the absorption in haemoglobin solutions have demonstrated a spectrum of relaxation times with the highest relaxation frequency on the order of at least 80 MHz (Edmonds 1962; Schneider et al. 1969; Edmonds et al. 1970). At physiological pH levels, one of the predominant relaxation mechanisms is thought to be due to a solute-solvent reaction in which particular side chains of histidine (one of the amino acids found in proteins) undergo a proton transfer reaction (Slutsky et al. 1980; Edmonds 1982; Holmes and Challis 1996). In solutions of haemoglobin, the overall relaxation absorption has been shown to be linearly dependent on the protein concentration (Schneider et al. 1969). The absorption in protein solutions has also been shown to be higher than that in the corresponding depolymorized solutions containing the constituent amino-acids and polypeptides (Kremkau and Cowgill 1984). However, due to the variety and complexity of the proteins involved, the specific details of the individual relaxation mechanisms that contribute to acoustic absorption in whole blood are still not well understood.

Absorption due to viscous relative motion occurs because of the difference in density between the intact red blood cells and the surrounding plasma (Carstensen and Schwan 1959a). This causes a cyclic transfer of momentum due to a phase difference between the oscillating cell and the compressional wave in the extracellular fluid (Epstein and Carhart 1953). This effect is increased if the cell size is reduced by increasing the tonicity of the suspension. (Blood cells will release water *via* osmosis in hypertonic environments due to the difference in the osmotic pressure across the cell membrane. This has the effect of increasing the cell density.) At low volume concentrations of red blood cells, the absorption due to viscous relative motion increases linearly as a function of concentration (Carstensen and Schwan 1959a). However, at high concentrations (beyond 40%–50% haematocrit), these effects are reduced due to interactions between the cells. At 1 MHz and physiological cell concentrations, losses due to viscous relative motion are thought to contribute on the order of 25% of the total attenuation in whole blood and 45% in suspensions of red blood cells in saline (Dai and Feng 1988; Zinin 1992). The contribution is higher in saline suspensions due to the increased density disparity between the interior of the cell and the extracellular fluid. At 10 MHz, the contribution of viscous relative motion is reduced to 5% in whole blood and 12% in saline suspensions of red blood cells and continues to decrease with increasing frequency. Measurements of the acoustic attenuation coefficient in haemoglobin solutions or solutions of hemolyzed red blood cells will consequently differ from those made in blood samples in which the cell membranes remain intact, particularly below 10 MHz (Carstensen 1972; Danckwerts and

Juergens 1977). Note, viscous relative motion can also be considered a relaxation process in which the relaxation time is itself a function of frequency (Bamber 2004).

On a cellular level, absorption due to thermal conduction (or heat flow) occurs because of the differing thermal parameters between the intracellular and extracellular fluids (Anson and Chivers 1990). This causes a temperature gradient across the cell membrane that leads to absorption by thermal diffusion. However, in comparison to the absorption due to viscous relative motion, the absorption due to thermal conduction is thought to be negligible, except at very low frequencies (Love and Kremkau 1980; Anson and Chivers 1989; Zinin 1992). On a molecular level, absorption due to thermal conduction occurs because the changes in acoustic pressure due the propagation of a compressional acoustic wave are not exactly adiabatic, nor isothermal. This results in heat flow from regions of higher temperature (pressure compressions where the average molecular motion is faster) to lower temperature regions (pressure rarefactions where the average molecular motion is slower) and a dissipation of acoustic energy. The corresponding thermal relaxation time can be estimated by $\tau_{therm}=\kappa/(\rho_0 c_0^2 \mathrm{C}_p)$, where κ is the thermal conductivity, ρ_0 is the density, c_0 is the sound speed and C_p is the heat capacity at constant pressure (Kinsler et al. 2000). Using the properties given by Ahuja (1974), the thermal relaxation times for water, plasma and red blood cells are all on the order of $6\times10^{-14}s$ (corresponding to a relaxation frequency on the order of 100 THz). Consequently, over the ultrasound frequency range of interest, the contribution of thermal conduction to attenuation can be considered negligible.

In addition to the dependence of ultrasound attenuation on the concentration of red blood cells and blood proteins, experimental results have also shown dependencies on the measurement temperature and the level of haemoglobin oxygenation. For example, Carstensen and Schwan (1959b) showed the attenuation coefficient at 10 MHz in solutions of human haemoglobin at 25°C and 15°C compared with 35°C increased by 7% and 18%, respectively. Similarly, Schneider et al. (1969) showed a 4% increase in the attenuation coefficient at 10 MHz in deoxygenated haemoglobin solutions compared with oxygenated solutions. However, at 500 MHz, they showed an 8% decrease for the same comparison. Shung and Reid (1977) showed a much greater increase (on the order of 60% at 10 MHz) for deoxygenated sickle cell blood and solutions of deoxyhaemoglobin S, but did not report the equivalent comparison for normal blood. Given the small variation in the oxygenation of whole blood *in vivo*, the effect of the oxygenation saturation on physiologically relevant attenuation measurements is likely to be small.

Contribution of scattering to attenuation measurements

Although ultrasound absorption may be quantified by directly measuring the amount of acoustic energy converted into thermal energy (*e.g.*, Fry and Fry 1954), most experimental techniques instead measure the total acoustic attenuation including the effects of scattering. In human blood, ultrasonic scattering is dependent on many factors, including haematocrit, frequency and flow conditions (see Shung and Thieme 1993 for a detailed overview). Below 10 MHz, the contribution of scattering to ultrasound attenuation in blood is negligible (Shung et al. 1976; Zinin 1992). However, due to the frequency dependence of the scattering (the blood cells behave approximately as Rayleigh scatterers below 30 MHz and thus the scattering scales with the fourth power of frequency), this contribution may become more significant at higher frequencies. For example, between 10 and 100 MHz, the backscattered power can increase by as much as three orders of magnitude (Fontaine and Cloutier 2003). If the scattering becomes a significant proportion of the experimentally measured attenuation, the idiosyncratic factors affecting the scattering will also become important. For example, scattering in whole blood is strongly dependent on the aggregation of red blood cells, which itself is dependent on the shear rate and the concentration of the plasma protein fibrinogin. Conversely, absorption at high frequencies is only dependent on the overall concentration of the various blood proteins. The exact quantification of the contribution of scattering to measurements of attenuation at higher frequencies remains an interesting open question.

METHODS

The ultrasound attenuation coefficient and dispersion in whole blood and its components were measured in transmission using a fixed path substitution technique (see Fig. 1). Test samples of approximately 150 mL were transferred to a glass beaker within a water bath. The samples were continuously pumped through 3 mm internal diameter plastic tubing into an oval-shaped test cavity (40 × 20 × 4.82 mm) using a rotary peristaltic pump. The arrangement of the inlet and outlet tubing allowed any air bubbles within the tubing circuit to be naturally vented. The temperature of the water bath was adjusted to maintain a temperature of 37 ± 0.5°C at the input to the test cavity as measured by a k-type thermocouple junction within the tubing. The flow speed was maintained at 1.7 mL/s for all tests. During circulation, broadband monopolar ultrasound plane wave pulses were continuously generated *via* thermo-elastic expansion by illuminating an optically absorbing black paint layer on one side of the test cavity with nanosecond laser

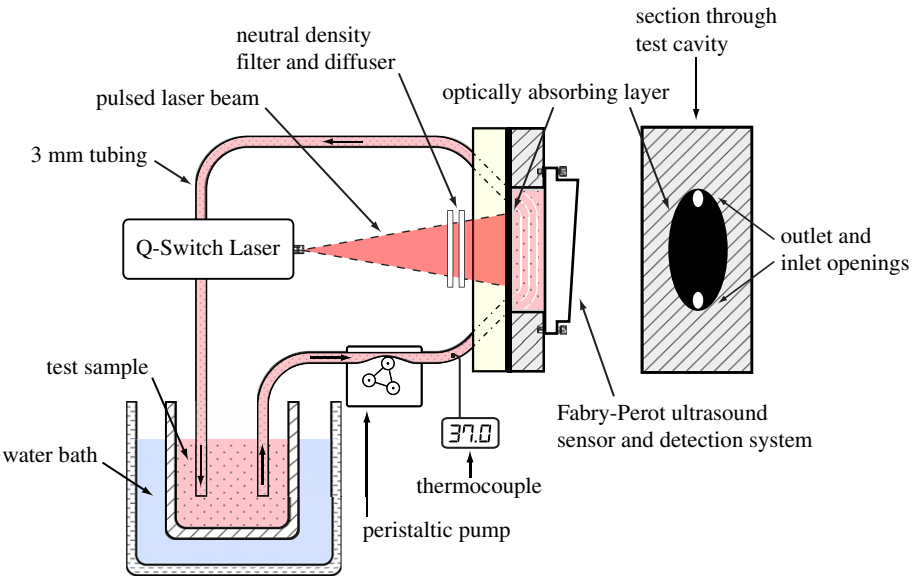

Fig. 1. Schematic of the experimental set-up used for the measurement of ultrasonic attenuation and dispersion. The test fluid is pumped from a water bath into an oval shaped test cavity via a peristaltic pump. Monopolar broadband ultrasound plane waves are generated in the cavity *via* thermoelastic expansion using nano-second laser pulses which illuminate an optically absorbing paint layer. The transmitted signals are then detected using a broadband Fabry-Perot interferometer.

pulses (Treeby et al. 2009). The thickness of the optically absorbing paint layer was sufficient such that the transmission of optical power through the layer was less than 2%. The laser source used was a Q-switched Nd:YAG (Ultra; Big Sky Laser Technologies, Bozeman, MT, USA) with a wavelength, pulse duration, pulse energy and repetition frequency of 1064 nm, 5.6 ns, 40 mJ and 20 Hz, respectively. The beam was homogenised by using a diffuser and the pressure of the generated ultrasound pulse was controlled by inserting various neutral density filters into the beam path. The ultrasound pulses were detected on the opposite side of the test cavity using a high-finesse Fabry-Perot interferometer made from two partially reflecting gold mirrors with a 7.5 μm parylene spacer (Zhang et al. 2008). The sensor transduction mechanism is based on acoustically induced changes in the optical thickness of the spacer. These changes modulate the reflectivity of the interferometer which is then detected by an additional focused laser beam incident on the sensor (Beard et al. 1999). The pressure signals were recorded at the centre of the test cavity using a time record of 400 ns, a sampling frequency of 5 GHz and 1000 averages. The measurements were triggered by a photodiode positioned near the laser output. The uniformity of the generated plane wave was tested by comparing the arrival time of the pressure peak over a 10×10 mm area around the central scan point. The maximum variation was on the order of 1 ns. Thus, for the purpose of acoustic measurements, the generated waves can be considered planar.

Before each test, a reference measurement was first made in deionized water (15 MΩ cm). The tubing circuit and test cavity were then emptied by reversing the pump and the test fluid added. A small quantity of the test fluid was purged from the circuit to ensure the sample was not diluted by any water remaining within the tubing or test cavity. All fluids were left to circulate for approximately ten minutes before testing to allow the temperature to equalise. The measurements in both the reference and test fluids were repeated three times, with each measurement taking 50 s to complete. The test fluid was then emptied into 50 mL syringes and weighed to allow the approximate measurement of the fluid density (20 mL syringes were used for the whole blood measurements due to the small volume of the samples). The tubing circuit was then purged for several minutes using deionized water. After each series of measurements, the circuit was also cleaned using a weak solution of isopropanol and then again purged with deionized water. No settling or coagulation of the blood was observed during the measurements.

To extract the attenuation coefficient and dispersion, the measurements were first averaged after removing any outliers due to fluctuations in the laser power outside the normal range. The amplitude and phase spectrums were then calculated using a circular-shifted fast Fourier transform as described by Treeby et al. (2009). These were used to calculate the attenuation and dispersion within the test fluid. The attenuation coefficient measurements were corrected for the absorption within the deionized

Table 2. Polynomial coefficients used to compute the absorption coefficient $\alpha_0(T)=a_0+a_1T+a_2T^2+\ldots+a_7T^7$ in dB MHz^{-2} cm^{-1} in deionized water as a function of temperature T in °C, where the total absorption in $dB\,cm^{-1}$ is given by $\alpha_0(T)f^2$

Coefficient	Value
$\mathbf{a_0}$	4.927006×10^{-3}
$\mathbf{a_1}$	-2.518622×10^{-4}
$\mathbf{a_2}$	8.621150×10^{-6}
$\mathbf{a_3}$	-1.795746×10^{-7}
$\mathbf{a_4}$	1.901728×10^{-9}
$\mathbf{a_5}$	$-5.394754 \times 10^{-12}$
$\mathbf{a_6}$	$-5.561328 \times 10^{-14}$
$\mathbf{a_7}$	3.360950×10^{-16}

The values are calculated from the data given by Pinkerton (1949).

water using a seventh-order polynomial fitted to the data given by Pinkerton (1949). The polynomial coefficients are given in Table 2. The bulk sound speed in the test fluid was calculated by using the relative arrival time of the signal maxima in the test and reference fluids along with the relationship for the temperature dependent speed of sound in water given by Marczak (1997). Power law parameters were obtained by simultaneously fitting a power law and the corresponding Kramers-Kronig relation to the attenuation and dispersion curves using an unconstrained nonlinear optimisation (Treeby et al. 2009). Examples of the recorded time signals and the corresponding amplitude spectrums in deionized water and whole blood are shown in Figure 2. The signal measured in blood arrives earlier due to a higher sound speed and the signal magnitude is visibly reduced due to attenuation. The corresponding attenuation parameters are presented up to 70 MHz (above this frequency the signal fidelity becomes significantly reduced). This upper limit is dependent on a combination of the strength of the ultrasound source, the attenuation within the test fluid, the thickness of the measurement cell, and the sensitivity and bandwidth of the Fabry-Perot ultrasound sensor.

Due to the difficulty in accurately calibrating the absolute pressure generated by the optically absorbing layer (the generated pulses were extremely broadband), the effect of non-linear wave propagation on the measured attenuation coefficient was quantified by repeating measurements with a gradually decreasing source strength. This was adjusted by using a range of neutral density filters in the beam path. After an asymptotic value for the attenuation coefficient was reached, this value for the neutral density filter was used for all remaining tests. The effect of varying the flow speed from 0 to 5 mL/s was also investigated using a saline solution of red blood cells with a total haemoglobin concentration of 15 g/dL. This variation had no noticeable effect on the measured attenuation coefficient.

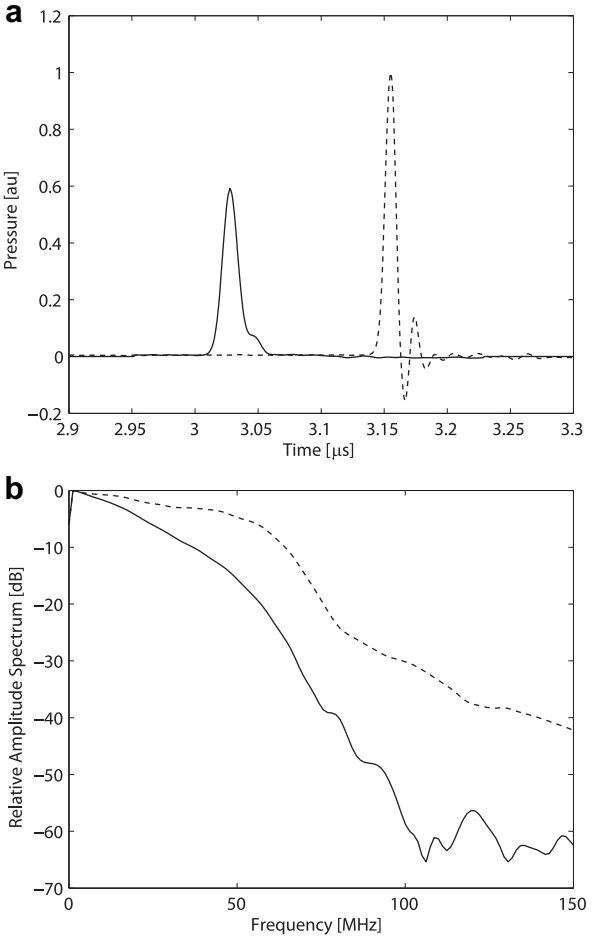

Fig. 2. Example of (a) the averaged pressure signals, and (b) the corresponding amplitude spectrums recorded in deionized water (dashed line) and whole blood (solid line).

RESULTS

Blood components

To test the ultrasound properties of individual blood components, recently expired blood products were obtained from the Department of Haematology and Blood Transfusion at University College London Hospital. Three products were used: (1) red cells in additive solution, leukocyte depleted, (2) red cells in additive solution, leukocyte depleted, for neonatal use and (3) fresh frozen plasma, leukocyte depleted (James and McClelland 2005; Kosmirak 2010). All tests were completed within 24 to 48 h of the product expiry, with the samples kept under the appropriate laboratory conditions. The red cells, collected in citrate phosphate dextrose (CPD) anticoagulant and suspended in 100 mL of additive solution (sodium chloride 150 mmols/L, adenine 1.25 mmols/L, anhydrous glucose 45.4 mmols/L, mannitol 28.8 mmols/L), were further diluted with phosphate buffered saline (P4417; Sigma-Aldrich, St. Louis, MO, USA) to give the desired haemoglobin concentration.

Table 3. Measured ultrasonic properties of whole blood and its components at 37°C

Component	c [m/s]	ρ [kg m^{-3}]	α_{0-70}	α_{0-15}
RBC in saline (10 g/dL)	1562 (0.7)	1036 (4.9)	$0.0106f^{1.88}$	$0.0475f^{1.47}$
RBC in saline (15 g/dL)	1576 (1.0)	1047 (5.6)	$0.0291f^{1.69}$	$0.0657f^{1.47}$
RBC in saline (20 g/dL)	1593 (1.0)	1058 (5.7)	$0.0596f^{1.56}$	$0.0798f^{1.49}$
Whole blood (15.1 g/dL)	1590 (2.8)	1049 (9.2)	$0.0546f^{1.58}$	$0.0596f^{1.56}$
Plasma	1553 (0.8)	1022 (2.6)	$0.0231f^{1.62}$	$0.0431f^{1.45}$
Phosphate buffered saline	1535 (2.7)	*997	–	–
Deionized water	*1524	*993	* $0.00139f^2$	* $0.00139f^2$

Here c is the sound speed, ρ is the density, α_{0-70} is the power law fit using the measured attenuation and dispersion data from 0-70 MHz in $dB\,\mathrm{cm}^{-1}$ and α_{0-15} is the analogous power law fit using the data from 0-15 MHz. Values given in brackets indicate standard deviation. The (*) denotes values from the literature, where the density in saline is taken from Kenner (1989), the sound speed and density in deionized water are taken from Marczak (1997) and Tanaka et al. (2001) and the absorption in deionized water is calculated using the polynomial coefficients given in Table 2. The sound speed and density values given for whole blood are taken from Table 4.

Three concentrations of total haemoglobin, 10, 15 and 20 g/dL (corresponding to approximate haematocrits of 30%, 45% and 60%) were investigated. The concentrations were measured using a calibrated co-oximeter (IL682; Instrumentation Laboratory, Bedford, MA, USA). Before dilution with phosphate buffered saline, the red cells for adult transfusion had a mean total haemoglobin concentration of 20.6 g/dL (0.9), while for the neonatal units this was 20.5 g/dL (0.8). (Values for the standard deviation are given in brackets.) The corresponding mean oxygenation saturation was 63.3% (10.2) for the adult units and 98.4% (0.4) for the neonatal units. Measurement of the oxygen saturation in several of the adult units after testing (which took approximately 20 min for each sample) illustrated an increase on the order of 10% to 15%. However, variations in the attenuation coefficient due to oxygen saturation were not observed in measurements repeated over this time or between samples with different oxygen saturations.

For each of the four test conditions (red blood cells in saline at three different concentrations and plasma), five different samples were tested. For each sample, the measurement was also repeated three times. The corresponding reference measurements were also repeated three times, giving a total of nine data set combinations per sample and 45 data sets per test condition. These were averaged and the average values used to fit the power law parameters. The resulting values for the sound speed, density and power law fits are given in Table 3. The corresponding values for the reference fluids taken from the literature are also given. The standard deviations for the density measurements (shown in brackets) correspond to a variation of approximately 0.25 mL in the volume of the measured sample. Both the sound speed and density for the red blood solutions in saline vary linearly with total haemoglobin concentration as expected, with the corresponding regression lines given by $c = 3.1 \times tHb[\mathrm{g}/dL] + 1531$ and $\rho = 2.21 \times tHb[\mathrm{g}/dL] + 1014$. Here c is the sound speed, ρ is the density and tHb is the total haemoglobin concentration. No difference in the attenuation coefficient was measured between the phosphate buffered saline and the deionized water.

The attenuation coefficient and dispersion measured in saline solutions of red blood cells with a total haemoglobin concentration of 15 g/dL are shown in Figure 3a–d. The upper plots show the data over the frequency range 0–70 MHz, and the lower plots show the same data over 0–15 MHz. The variation in the attenuation coefficient and dispersion with the concentration of red blood cells for total haemoglobin concentrations of 10, 15 and 20 g/dL are shown in Figure 3e and f. The corresponding power law parameters are listed in Table 3. The large error bars in the dispersion plots are due to small variations in the haemoglobin concentration and temperature between each measurement sample. These variations have the effect of vertically translating the dispersion curve (as the overall sound speed in the medium changes). However, the shapes of the measured dispersion curves from the individual data sets closely match that of the mean. The positive gradient of the dispersion curves shown in Figure 3f suggests the distribution of relaxation frequencies extends beyond the current range of measurement frequencies, consistent with observations made in previous studies (Schneider et al. 1969).

While it is common in the literature to characterise the acoustic attenuation coefficient in biologic tissues by a single power law (*e.g.*, Duck 1990; Szabo 2004), this approach is not necessarily justified for describing the attenuation coefficient over a broad frequency range due to the varying frequency dependence of the different mechanisms involved. For example, while the 0–70 MHz power law fit shown in Figure 3 closely matches the attenuation coefficient and dispersion measured above 20 MHz, at lower frequencies the measured attenuation coefficient is noticeably higher. Similarly, the 0–15 MHz power law fit, which closely

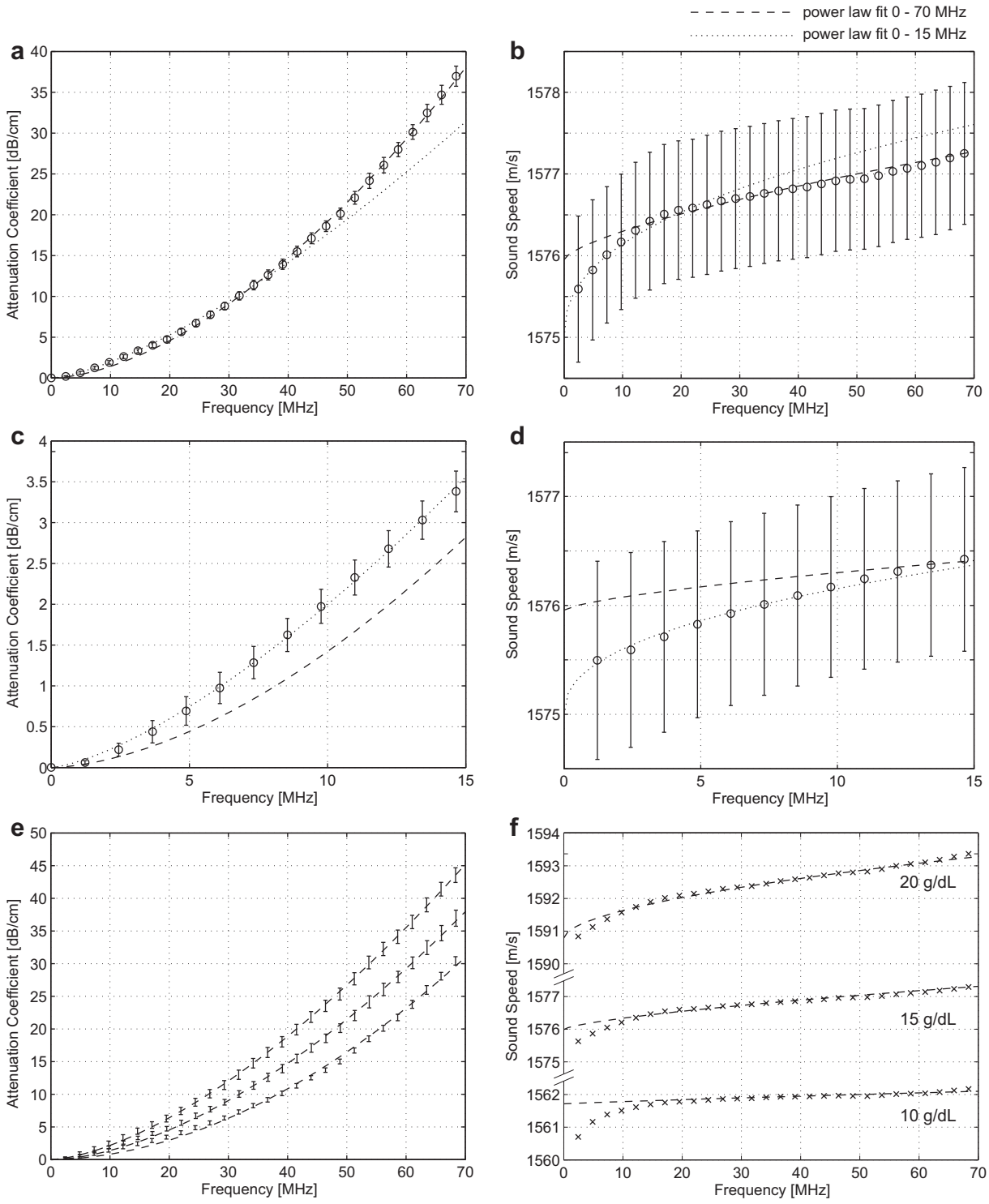

Fig. 3. (a)–(d) Attenuation coefficient and dispersion measured at 37°C in solutions of human red blood cells in saline with a total haemoglobin concentration of 15 g/dL. The circles and error bars show the mean and standard deviation of the experimental measurements, and the dashed and dotted lines show power law fits using the data from 0–70 and 0–15 MHz, respectively. (e)–(f) Variation in the measured attenuation coefficient and dispersion with changes in the total haemoglobin concentration from 10 g/dL (lower curves) to 20 g/dL (upper curves).

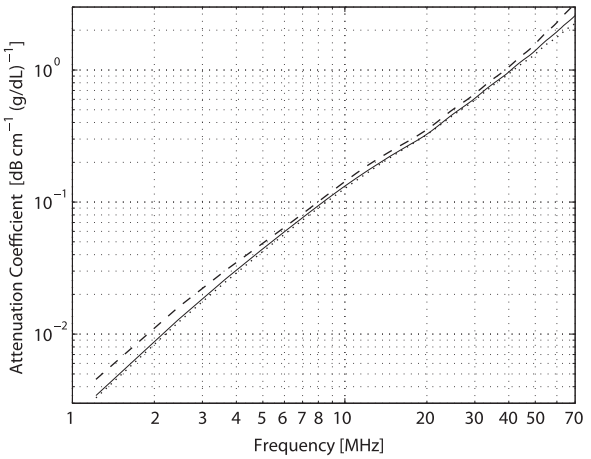

Fig. 4. Concentration normalised attenuation coefficient measured at 37°C for solutions of human red blood cells in saline. The dashed line corresponds to measurements made at 10g/dL, the solid line at 15 g/dL, and the dotted line at 20 g/dL.

follows the measured attenuation coefficient and dispersion at lower frequencies, cannot be extrapolated to describe the behaviour at higher frequencies. It is likely that this disparity is due to the additional absorption provided at lower frequencies due to viscous relative motion. This is also evident in Figure 4 which shows the concentration normalised attenuation coefficient for the three tested concentrations of red blood cell solutions on a logarithmic plot. The exponent of the power law (in this case the gradient of the line) varies gradually with frequency, particularly below 20 MHz. At very high frequencies, the attenuation coefficient for a total haemoglobin concentration of 10 g/dL also appears to increase more rapidly than at the other concentrations. It is possible this is due to an increased contribution from scattering (the scattering has a negative parabolic dependence on haematocrit, with the maximum in the region of 15%, Shung and Thieme 1993). A dependence of the power law exponent on frequency has also been noted for many other biologic tissues, including haemoglobin (Bamber 2004). Consequently, while a power law provides an extremely convenient way to summarise and model experimentally measured variations of attenuation coefficient and dispersion (for example Treeby and Cox 2010), it would be prudent to exercise caution before assigning particular significance to the precise values of the power law parameters themselves.

Whole blood

To test the ultrasound properties of whole blood, a 40 mL sample of venous blood was taken *via* venipuncture from four healthy adult volunteers aged 26 to 35 (three male and one female). The study was approved by The Joint UCL/ULCH Committees on the Ethics of Human

Table 4. Properties of venous blood taken from four healthy adult volunteers measured at 37°C

Subject	tHb [g/dL]	c [m/s]	ρ [kg m^{-3}]
S1	15.1	1590	1052
S2	15.2	1591	1060
S3	14.1	1587	1039
S4	15.9	1593	1044
Mean	15.1 (0.74)	1590 (2.8)	1049 (9.2)

Here tHb is the total haemoglobin concentration, c is the sound speed and ρ is the density. Values given in brackets indicate standard deviation.

Research and informed consent for the study was obtained from all human subjects. The blood was collected in ethylenediaminetetraacetic acid (EDTA) anticoagulant in 4 mL purple top Vacutainers (Becton, Dickinson and Company, Franklin Lakes, NJ, USA) and then refrigerated. Both EDTA and CPD work by chelating calcium which is required for clotting. All tests were completed within 4 h of donation. The haemoglobin level, sound speed, and density for each subject are given in Table 4. Due to the small volume of the samples and the measurement method

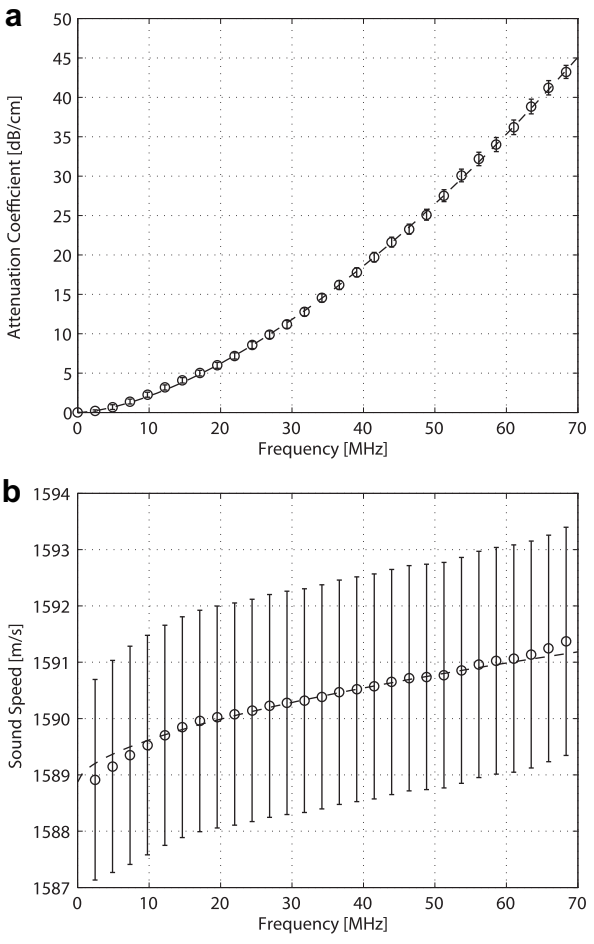

Fig. 5. Attenuation coefficient and dispersion measured at 37°C in whole human blood with an average total haemoglobin concentration of 15 g/dL.

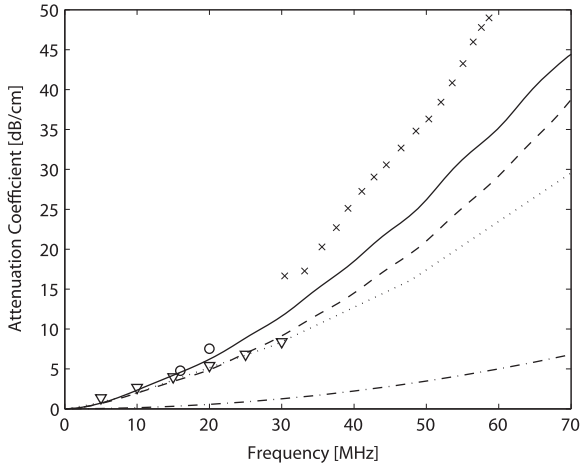

Fig. 6. Comparison of broadband blood attenuation coefficient measurements reported in the literature. Crosses: human red blood cells (RBC) in saline (Lockwood et al. 1991); solid line: whole human blood (from Fig. 5); dashed line: human RBC in saline (from Fig. 3); dotted line: bovine haemoglobin in water (Edmonds et al. 1970); triangles: porcine RBC in saline (Wang and Shung, 1997); open circles: whole blood (Secomski et al. 2001); dash-dot line: water absorption.

used, the uncertainty in the density measurements is on the order of ± 12.5 kg m^{-3} (± 0.25 mL). The average attenuation coefficient and dispersion are shown in Figure 5. Although the mean total haemoglobin concentration is 15.1 g/dL, the attenuation coefficient is greater than that measured in the corresponding solution of red blood cells and saline. This is due to the presence of additional proteins within the blood plasma that contribute to relaxation absorption. The 0–70 MHz power law fit also matches the measured lower frequency data more closely than the corresponding fits for suspensions of red blood cells in saline. This is consistent with a reduction in the effect of absorption due to viscous relative motion (the density difference between the intracellular fluid and the plasma is less than between the intracellular fluid and the saline).

Comparison to previously reported measurements

A comparison of the broadband measurements of ultrasound attenuation coefficient reported here with those previously reported in the literature is shown in Figure 6. Where papers have reported measurements under multiple conditions, the values closest to 15 g/dL (45% haematocrit) and 37°C have been used (see Table 1). Below 30 MHz, there is a good agreement between the measurements reported by Wang and Shung (1997) for solutions of porcine red blood cell (RBC) in saline, the measurements reported by Edmonds et al. (1970) for aqueous solutions of bovine haemoglobin, and the measurements reported here for solutions of red blood cells in saline (the displayed data are all for a total haemoglobin concentration of 15 g/dL). At higher frequencies, the attenuation coefficient measured here for red blood cell suspensions becomes higher than that measured in haemoglobin suspensions. This could be due to the contribution of scattering from the red blood cells. The attenuation coefficient in the whole blood and blood cell suspensions measured here are both significantly less than the experimental data presented by Lockwood et al. (1991). As the latter were made in the context of characterising ultrasonic backscatter and the acoustic pressures used are not reported, it is possible that this difference is due to the effects of nonlinear wave propagation (a detailed discussion of the various sources of error in attenuation measurements is given by Bamber 2004).

Historically, the attenuation coefficient in blood is commonly cited as varying with $0.14f^{1.21}$ (these parameters appear in several reference texts, for example Duck 1990; Szabo 2004). However, analogous to earlier discussion such equations only have a limited range of validity due to the varying frequency dependence of the different attenuation mechanisms. For example, the attenuation coefficient predicted by this equation at 70 MHz is approximately 20 dB less than that measured here for whole blood. It is interesting to note that at 70 MHz the absorption in water (dash-dot line in Fig. 6) is 6.8 dB and thus cannot be neglected from the calculation of the attenuation coefficient.

The values of sound speed and density reported here are in good agreement with those presented previously. For example, Secomski et al. (2001) reported a regression line of $c = 0.9 \times HCT[\%] + 1545$ for the sound speed in whole blood at 37°C using the data from 168 volunteers (here HCT is the haematocrit). For a haematocrit of 45%, this gives a sound speed of 1586 m/s, which is close to the average value reported here for whole blood of 1590 m/s. Similarly, using the density data provided by Kenner (1989), a regression line may be given as $\rho = 0.78 \times HCT[\%] + 1017$. For a haematocrit of 45% this gives a density value of 1052 kg m^{-3} which is again very close to the average value reported here for whole blood of 1049 kg m^{-3}.

SUMMARY AND DISCUSSION

The ultrasonic attenuation coefficient and dispersion in whole blood, suspensions of red blood cells in saline and plasma have been reported. The measured power law dependence is shown to vary across the investigated frequency range, particularly below 20 MHz. This may be attributed to the varying frequency dependence of the different mechanisms that contribute to the measured attenuation coefficient (for example, relaxation absorption and viscous relative motion). This makes it difficult

to assign a single power law to accurately describe the attenuation coefficient at all frequencies of interest. However, for the purpose of modelling the attenuation of broadband acoustic waves, using a single power law is both conceptually and computationally simpler and may be sufficient to capture the properties of interest (Treeby and Cox 2010).

In the current article, the experimental attenuation and dispersion data are presented up to 70 MHz. This upper limit (determined by the available signal fidelity) is dependent on a combination of the strength of the ultrasound source, the attenuation within the test fluid, the thickness of the measurement cell, and the sensitivity and bandwidth of the Fabry-Perot ultrasound sensor. Either of the latter two parameters could potentially be adjusted to increase the measurement bandwidth (the development of high sensitivity broadband Fabry-Perot intereferometers remains the subject of ongoing work). Similarly, if high fidelity measurements at lower frequencies are a priority, the sample thickness could be increased.

Although reference measurements made using the presented optical measurement technique have not been compared to those made using other techniques over the complete frequency range presented, previous comparisons at lower frequencies using castor oils have shown good quantitative agreement (Treeby et al. 2009). The current methodology also mitigates many of the common errors that afflict attenuation coefficient measurements (Bamber 2004). For example, the planar transducers can accurately measure dispersion, there are no focusing or diffraction errors, the temperature and flow speed within the measurement cell can be easily regulated, and there are no sample dependent reflections which are present when using insertion techniques. However, some possible sources of measurement error remain. The difference in the characteristic impedance between the test and reference fluids may cause variations in the transmission efficiency of the acoustic wave into the sensor (estimated to be at most 3%). If the acoustic absorption within the deionised water used as the reference fluid differs from that reported by Pinkerton (1949), this will also cause a systematic error in the reported attenuation coefficients. However, for the fluids tested here, the water absorption accounts for at most 15% of the attenuation coefficient, thus a 1% variation in the absorption in the reference fluid would manifest as a 0.15% error in the measured attenuation coefficient.

It would be interesting in the future to repeat these measurements with suspensions of lysed red blood cells. This would allow the contribution of the attenuation mechanisms dependent on the intact cell membrane (viscous relative motion and scattering) to be more formally investigated. Similarly, it would be interesting to use the current measurement system to perform a systematic investigation into the effect of temperature on the measured attenuation coefficient and dispersion, similar to that previously reported for olive and castor oils (Treeby et al. 2009). It may also be possible to perform the experiments in both transmission and reflection modes to allow the simultaneous characterisation of attenuation and backscatter.

Acknowledgments—The authors would like to thank Paul Beard, Jan Laufer and Thomas Allen for useful discussion. This work was supported by the Engineering and Physical Sciences Research Council, UK.

REFERENCES

Ahuja A. Measurement of thermal conductivity of stationary blood by unsteady-state method. J Appl Physiol 1974;37:765.

Anson L, Chivers R. Ultrasonic propagation in mammalian cell suspensions based on a shell model. Phys Med Biol 1989;34:1153–1167.

Anson LW, Chivers RC. Thermal effects in the attenuation of ultrasound in dilute suspensions for low values of acoustic radius. Ultrasonics 1990;28:16–26.

Bain BJ. Blood cells: A practical guide. Malden: Blackwell Publishing; 2006.

Bamber JC. Attenuation and absorption. In: Hill CR, Bamber JC, ter Haar GR, (eds). Physical principles of medical ultrasonics. Chichester: John Wiley and Sons Ltd; 2004. p. 93–166.

Barnes C, Evans JA, Lewis TJ. Low-frequency ultrasound absorption in aqueous solutions of hemoglobin, myoglobin, and bovine serum albumin: The role of structure and pH. J Acoust Soc Am 1988;83: 2393–2404.

Beard PC, Perennes F, Mills TN. Transduction mechanisms of the Fabry-Perot polymer film sensing concept for wideband ultrasound detection. IEEE Trans Ultrason Ferroelectr Freq Control 1999;46: 1575–1582.

Carstensen EL. Effects of hemolysis on ultrasonic absorption in blood. Acustica 1972;25:183.

Carstensen EL, Li K, Schwan HP. Determination of the acoustic properties of blood and its components. J Acoust Soc Am 1953;25: 286–289.

Carstensen EL, Schwan HP. Absorption of sound arising from the presence of intact cells in blood. J Acoust Soc Am 1959a;31:185–189.

Carstensen EL, Schwan HP. Acoustic properties of hemoglobin solutions. J Acoust Soc Am 1959b;31:305–311.

Dai H, Feng R. Ultrasonic attenuation in red blood cell suspensions. Ultrasonics 1988;26:168–170.

Danckwerts HJ, Juergens KD. Ultrasonic investigations of hemolysis. Ultrasound Med Biol 1977;2:339–341.

Duck FA. Physical properties of tissue: A comprehensive reference book. London: Academic Press; 1990.

Dukhin AS, Goetz PJ, van de Ven TGM. Ultrasonic characterization of proteins and blood cells. Colloid Surf. B-Biointerfaces 2006;53: 121–126.

Edmonds PD. Ultrasonic absorption of haemoglobin solutions. Biochim Biophys Acta 1962;63:216–219.

Edmonds PD. The molecular basis of ultrasonic absorption by proteins. Bioelectromagnetics 1982;3:157–165.

Edmonds PD, Bauld TJ, Dyro JF, Hussey M. Ultrasonic absorption of aqueous hemoglobin solutions. Biochim Biophys Acta 1970;200: 174–177.

Epstein PS, Carhart RR. The absorption of sound in suspensions and emulsions. I. Water fog in air. J Acoust Soc Am 1953;25:553–565.

Fairbanks VF, Tefferi A. Normal ranges for packed cell volume and hemoglobin concentration in adults: Relevance to “apparent polycythemia”. Eur J Haematol 2000;65:285–296.

Fairbanks VF, Tefferi A. Letter to the Editor. Eur J Haematol 2001;67: 203–204.

Fontaine I, Cloutier G. Modeling the frequency dependence (5–120 MHz) of ultrasound backscattering by red cell aggregates in shear flow at a normal hematocrit. J Acoust Soc Am 2003;113:2893–2900.
Foster FS, Pavlin CJ, Harasiewicz KA, Christopher DA, Turnbull DH. Advances in ultrasound biomicroscopy. Ultrasound Med Biol 2000;26:1–27.
Francois RE, Garrison GR. Sound absorption based on ocean measurements: Part I: Pure water and magnesium sulfate contributions. J Acoust Soc Am 1982;72:896–907.
Fry WJ, Fry RB. Determination of absolute sound levels and acoustic absorption coefficients by thermocouple probes—experiment. J Acoust Soc Am 1954;26:311–317.
Giacomini A, Legovini P, Gessoni G, Antico F, Valverde S, Salvadego M, Manoni F. Platelet count and parameters determined by the Bayer ADVIATM 120 in reference subjects and patients. Clin Lab Haematol 2001;23:181–186.
Hall L. The origin of ultrasonic absorption in water. Phys Rev 1948; 73:775.
Herzfeld KF, Rice FO. Dispersion and absorption of high frequency sound waves. Phys Rev 1928;31:691.
Holmes AK, Challis RE. Acoustic absorption due to proton transfer in solutions of proteins, peptides and amino acids at neutral pH. J Acoust Soc Am 1996;100:1865–1877.
Hoskins PR. Physical properties of tissues relevant to arterial ultrasound imaging and blood velocity measurement. Ultrasound Med Biol 2007;33:1527–1539.
Huang CC, Wang SH, Tsui PH. Detection of blood coagulation and clot formation using quantitative ultrasonic parameters. Ultrasound Med Biol 2005;31:1567–1573.
Hughes D, Geddes L, Babbs C, Bourland J, Newhouse V. Attenuation and speed of 10 MHz ultrasound in canine blood of various packed-cell volumes at 37°C. Med Biol Eng Comput 1979;17: 619–622.
Hughes MS, Marsh JN, Hall CS, Fuhrhop RW, Lacy EK, Lanza GM, Wickline SA. Acoustic characterization in whole blood and plasma of site-targeted nanoparticle ultrasound contrast agent for molecular imaging. J Acoust Soc Am 2005;117:964–972.
James V, McClelland B. Guidelines for the blood transfusion services in the United Kingdom. London: The Stationery Office; 2005.
Kenner T. The measurement of blood density and its meaning. Basic Res Cardiol 1989;84:111–124.
Kikuchi Y, Okuyama D, Kasai C, Yoshida Y. Measurements on the sound velocity and the absorption of human blood in 1-10 MHz frequency range (In Japanese). Record Semin Tohoku Univ 1972; 41:152–159.
Kinsler LE, Frey AR, Coppens AB, Sanders JV. Fundamentals of acoustics. 4th edition. New York: John Wiley and Sons; 2000.
Kosmirak L. Portfolio of blood components and guidance for their clinical use. NHS Blood Transplant 2010;SPECIFICATION SPN223/2.1.
Kremkau FW. Biomolecular absorption of ultrasound. III. Solvent interactions. J Acoust Soc Am 1988;83:2410–2415.
Kremkau FW, Carstensen EL, Aldridge WG. Macromolecular interaction in the absorption of ultrasound in fixed erythrocytes. J Acoust Soc Am 1973;53:1448–1451.
Kremkau FW, Cowgill RW. Biomolecular absorption of ultrasound. I: Molecular weight. J Acoust Soc Am 1984;76:1330–1335.
Kremkau FW, Cowgill RW. Biomolecular absorption of ultrasound: II. Molecular structure. J Acoust Soc Am 1985;77:1217–1221.
Libgot-Callé R, Plag C, Patat F, Ossant F. Interest of the attenuation coefficient in multiparametric high frequency ultrasound investigation of whole blood coagulation process. J Acoust Soc Am 2009; 125:530–538.
Liebermann LN. The second viscosity of liquids. Phys Rev 1949;75: 1415.
Liu Y, Maruvada S, Herman BA, Harris GR. Egg white as a blood coagulation surrogate. J Acoust Soc Am 2010;128:480–489.
Lockwood GR, Ryan LK, Hunt JW, Foster FS. Measurement of the ultrasonic properties of vascular tissues and blood from 35–65 MHz. Ultrasound Med Biol 1991;17:653–666.
Love LA, Kremkau FW. Intracellular temperature distribution produced by ultrasound. J Acoust Soc Am 1980;67:1045–1050.
Marczak W. Water as a standard in the measurements of speed of sound in liquids. J Acoust Soc Am 1997;102:2776–2779.
Maruvada S, Shung KK, Wang SH. High-frequency backscatter and attenuation measurements of porcine erythrocyte suspensions between 30–90 MHz. Ultrasound Med Biol 2002;28:1081–1088.
Narayana PA, Ophir J, Maklad NF. The attenuation of ultrasound in biological fluids. J Acoust Soc Am 1984;76:1–4.
O'Brien WD Jr, Dunn F. Ultrasonic absorption mechanisms in aqueous solutions of bovine hemoglobin. J Phys Chem 1972;76:528–533.
Pinkerton JMM. The absorption of ultrasonic waves in liquids and its relation to molecular constitution. Proc Phys Soc B 1949;62:129–141.
Schneck DJ. An outline of cardiovascular structure and function. In: Mudry KM, Plonsey R, Bronzino JD, (eds). Biomedical imaging. Boca Raton: CRC Press; 2003. p. 1–12.
Schneider F, Müller-Landau F, Mayer A. Acoustical properties of aqueous solutions of oxygenated and deoxgenated hemoglobin. Biopolymers 1969;8:537–544.
Secomski W, Nowicki A, Tortoli P. Estimation of hematocrit by means of attenuation measurement of ultrasonic wave in human blood. Proc IEEE Ultrason Symp 2001;2:1277–1280.
Secomski W, Nowicki A, Tortoli P, Olszewski R. Multigate Doppler measurements of ultrasonic attenuation and blood hematocrit in human arteries. Ultrasound Med Biol 2009;35:230–236.
Shung K, Reid J. The acoustical properties of deoxygenated sickle cell blood and hemoglobin S solution. Ann Biomed Eng 1977;5: 150–156.
Shung KK, Reid JM. Ultrasonic instrumentation for hematology. Ultrason Imaging 1979;1:280–294.
Shung KK, Sigelmann RA, Reid JM. Scattering of ultrasound by blood. IEEE Trans Biomed Eng 1976;BME-23:460–467.
Shung KK, Thieme GA, (eds). Ultrasonic scattering in biological tissue. Boca Raton: CRC Press; 1993.
Slutsky L, Madsen L, White R, Harkness J. Kinetics of the exchange of protons between hydrogen phosphate ions and a histidyl residue. J Phys Chem 1980;84:1325–1329.
Stride E, Saffari N. Theoretical and experimental investigation of the behaviour of ultrasound contrast agent particles in whole blood. Ultrasound Med Biol 2004;30:1495–1509.
Szabo TL. Diagnostic ultrasound imaging. London: Elsevier Academic Press; 2004.
Tanaka M, Girard G, Davis R, Peuto A, Bignell N. Recommended table for the density of water between 0°C and 40°C based on recent experimental reports. Metrologia 2001;38:301.
ter Haar G, Coussios C. High-intensity focused ultrasound: physical principles and devices. Int J Hyperthermia 2007;23:89–104.
Treeby BE, Cox BT. Modeling power law absorption and dispersion for acoustic propagation using the fractional Laplacian. J Acoust Soc Am 2010;127:2741–2748.
Treeby BE, Cox BT, Zhang EZ, Patch SK, Beard PC. Measurement of broadband temperature-dependent ultrasonic attenuation and dispersion using photoacoustics. IEEE Trans Ultrason Ferroelectr Freq Control 2009;56:1666–1676.
Treeby BE, Zhang EZ, Cox BT. Photoacoustic tomography in absorbing acoustic media using time reversal. Inverse Prob 2010;26:115003.
Wang SH, Shung KK. An approach for measuring ultrasonic backscattering from biological tissues with focused transducers. IEEE Trans Biomed Eng 1997;44:549–554.
White RD, Slutsky LJ. Ionization kinetics in aqueous solutions of bovine hemoglobin. J. Colloid Interface Sci 1971;37:727–730.
White RD, Slutsky LJ. Ultrasonic absorption and relaxation spectra in aqueous bovine hemoglobin. Biopolymers 1972;11:1973–1984.
Woodcock JP. Ultrasonic absorption–A new technique. Ultrasonics 1970;8:213–215.
Yuan YW, Shung KK. Ultrasonic backscatter from flowing whole blood. II: Dependence on frequency and fibrinogen concentration. J Acoust Soc Am 1988;84:1195–1200.
Zhang EZ, Laufer JG, Beard PC. Backward-mode multiwavelength photoacoustic scanner using a planar Fabry-Perot polymer film ultrasound sensor for high-resolution three-dimensional imaging of biological tissues. Appl Optics 2008;47:561–577.
Zinin PV. Theoretical analysis of sound attenuation mechanisms in blood and in erythrocyte suspensions. Ultrasonics 1992;30:26–34.